Search for the Pygmy Dipole Resonance in ^{68}Ni at 600 MeV/nucleon

O. Wieland,[1] A. Bracco,[1,2] F. Camera,[1,2] G. Benzoni,[1] N. Blasi,[1] S. Brambilla,[1] F. C. L. Crespi,[1,2] S. Leoni,[1,2] B. Million,[1] R. Nicolini,[1,2] A. Maj,[3] P. Bednarczyk,[3] J. Grebosz,[3] M. Kmiecik,[3] W. Meczynski,[3] J. Styczen,[3] T. Aumann,[4] A. Banu,[4] T. Beck,[4] F. Becker,[4] L. Caceres,[4,*] P. Doornenbal,[4,†] H. Emling,[4] J. Gerl,[4] H. Geissel,[4] M. Gorska,[4] O. Kavatsyuk,[4] M. Kavatsyuk,[4] I. Kojouharov,[4] N. Kurz,[4] R. Lozeva,[4] N. Saito,[4] T. Saito,[4] H. Schaffner,[4] H. J. Wollersheim,[3] J. Jolie,[5] P. Reiter,[5] N. Warr,[5] G. deAngelis,[6] A. Gadea,[6] D. Napoli,[6] S. Lenzi,[7,8] S. Lunardi,[7,8] D. Balabanski,[9,10] G. LoBianco,[9,10] C. Petrache,[9,‡] A. Saltarelli,[9,10] M. Castoldi,[11] A. Zucchiatti,[11] J. Walker,[12] and A. Bürger[13,§]

[1]INFN Sezione di Milano, I-20133 Milano, Italy
[2]Dipartimento di Fisica, Universitá di Milano, I-20133 Milano, Italy
[3]Institute of Nuclear Physics, Polish Academy of Sciences, 31-342 Kraków, Poland
[4]GSI, D-64291 Darmstadt, Germany
[5]Institut für Kernphysik, Universität zu Köln, D-50937 Köln, Germany
[6]Laboratori Nazionali di Legnaro, INFN, I-35020 Legnaro, Italy
[7]Dipartimento di Fisica, Universitá di Padova, I-35122 Padova, Italy
[8]INFN Sezione di Padova, I-35122 Padova, Italy
[9]Dipartimento di Fisica, Universitá di Camerino, I-62032 Camerino, Italy
[10]INFN Sezione di Perugia, I-06123 Perugia, Italy
[11]INFN Sezione di Genova, I-16146 Genova, Italy
[12]University of Surrey, Guildford, Surrey, GU2 7XH, United Kingdom
[13]HISKP, Universität Bonn, D-53115 Bonn, Germany
(Received 19 September 2008; published 4 March 2009)

The γ decay from Coulomb excitation of ^{68}Ni at 600 MeV/nucleon on a Au target was measured using the RISING setup at the fragment separator of GSI. The ^{68}Ni beam was produced by a fragmentation reaction of ^{86}Kr at 900 MeV/nucleon on a ^{9}Be target and selected by the fragment separator. The γ rays produced at the Au target were measured with HPGe detectors at forward angles and with BaF_2 scintillators at backward angles. The measured spectra show a peak centered at approximately 11 MeV, whose intensity can be explained in terms of an enhanced strength of the dipole response function (pygmy resonance). Such pygmy structure has been predicted in this unstable neutron-rich nucleus by theory.

DOI: 10.1103/PhysRevLett.102.092502 PACS numbers: 24.30.Gd, 25.70.De, 27.50.+e

The electric dipole ($E1$) response of nuclei at energies around the particle separation energy is presently attracting a lot of attention, particularly for unstable neutron-rich nuclei produced as radioactive beams. One of the important aspects in this connection is that the dipole strength distribution affects reaction rates in astrophysical scenarios where photodisintegration reactions are important, i.e., in hot stars and stellar explosions [1]. The accumulation of $E1$ strength around the particle separation energy is commonly denoted by the pygmy dipole resonance (PDR) due to the minor size of its strength in comparison with the giant dipole resonance which dominates the $E1$ response, and exhausts the Thomas-Reiche-Kuhn (TRK) oscillator sum rule. In the case of stable nuclei extensive work has been done ([2,3] and references therein) with photon scattering experiments in different mass regions and in general it is seen that the low energy $E1$ strength (below and around the neutron binding energy) is larger than that due to the tail of the giant dipole resonance (GDR). It is also found that this low energy strength increases with the N/Z ratio. Qualitatively, this increase has been explained as due to the vibration of the neutron skin. The problem of how the $E1$ strength evolves for nuclei far from stability in the neutron-rich side is presently one of the interesting topics in nuclear structure since it provides information on the properties of the neutron skin and on the nuclear equation of state for asymmetric nuclear matter, relevant for the study of neutron stars [4]. In particular, it is presently theoretically under discussion to which extent pygmy resonances represent a collective vibration of excess neutrons against an isospin-symmetric core [5]. For nuclei far from stability the pygmy dipole resonance was investigated using the heavy-ion induced electromagnetic excitation process at high beam energies. Low-lying dipole strength in the energy region below the GDR has been observed in the oxygen isotopes $^{20-22}$O [6,7] and in several neutron-rich nuclei around ^{132}Sn [8]. The unstable nucleus ^{68}Ni represents a good case to search for pygmy structures. This nucleus is located in the middle of the long isotopic Ni chain having at the extremes the doubly magic ^{56}Ni and ^{78}Ni and is experimentally accessible with the present radioactive beam facilities. In addition, different theoretical predictions on the pygmy dipole strength are available for this mass region [9–11]. The present Letter reports on the first search of the pygmy dipole resonance in ^{68}Ni using the virtual photon scattering technique at 600 MeV/nucleon, at which the excitation of vibrations of electric dipole character is dominating over other excitation modes [12].

The ^{68}Ni beam was produced from the fragmentation of ^{86}Kr beam from SIS at GSI at 900 MeV/nucleon with an intensity of $\sim 10^{10}$ particles per 6 s spill (10 s repetition rate) and focused on a 4 g/cm^2 thick ^{9}Be target. The ^{68}Ni ions were selected together with few other ions using the fragment separator (FRS [13]). A total of approximately 3×10^7 ^{68}Ni events were collected. The upper panel of Fig. 1 displays the selected and well separated ions. The ^{68}Ni ions are the most intense component (33% of the beam cocktail) impinging on the Au target (2 g/cm^2 thick). The particle identification after the Au target was performed by a calorimeter (CATE) [14,15] placed at 0°. It consisted of nine thin position sensitive Si detectors in front of four 6 cm thick CsI detectors, arranged symmetrically with respect to the beam. The opening angle θ of CATE is $\pm 2.0°$, which is much larger than the grazing angle of 0.43°. The total energy and energy loss correlation of events measured in CATE and corresponding to ^{68}Ni ions are shown in the middle panel of Fig. 1. The FWHM of the measured total energy peak is approximately 1% and therefore the present resolution is sufficient to discriminate between different masses of the outgoing nuclei. The γ-ray emission at the target location was measured using a specific configuration of the RISING setup [14]. Gamma rays were detected at different angles, at 16°, 33°, and 36° with the 15 HPGe clusters of the RISING array [16], at 51° and 88° with 7 HPGe segmented clusters of the Miniball [17] array and at 88° and 142° with 8 BaF_2 of the HECTOR array [18]. An important requirement to obtain γ-ray spectra from the measured data is to determine the v/c of the γ emitting nuclei on an event by event basis by tracking their trajectories before and after the Au target interaction. This is particularly important for large values of v/c as in the case of this experiment having $v/c \approx 0.79$ and a thick target. In fact, the target thickness induces a spread in the v/c value of $\approx 1\%$. In addition, all the γ-ray spectra here discussed are associated to ^{68}Ni scattered at $\theta \leq 0.43°$ to select Coulomb excitation [14]. In addition, the events used for the following analysis had γ multiplicity equal to one, corresponding to one γ-ray detector firing out of the 30 available. This is to reduced high multiplicity background events. The γ-ray energy spectrum measured with the HPGe RISING cluster detectors is shown for the high-energy region in Fig. 1 (lower panel). In order to check whether or not the measured structure at around 11 MeV could be due to γ transitions in a narrow peak emitted by the projectile, a GEANT [19] simulation was made. The simulation corresponded to a γ transition of 11 MeV from a moving source and included the source and detection conditions. In particular, the angular and energy straggling of the projectile in the target and the relativistic effects depending on position and opening angle of the detector were included. The result of the simulation, shown in the bottom panel of Fig. 1 by the continuous line, reproduces rather well the measured peak structure. An additional way to confirm that the peak structure at 11 MeV is originating from the deexcitation of ^{68}Ni projectile is to verify the angular dependence of the Doppler correction of the fast moving emitting source. The spectrum measured with BaF_2 detectors at 88° and corrected for the projectile velocity (Fig. 2) clearly shows a peak at 11 MeV. The cross section values were deduced by measuring singles events, not requiring γ detection, in the CATE calorimeter and by computing the γ detection efficiency of the array taking into account the γ angular distributions as given by the Lorentz boost. Also in this BaF_2 detector spectrum a peak structure is present at around 11 MeV. The error bars reflect the statistical error and the uncertainty in the determination of the value of v/c. In the inset of the figure the peak region of the BaF_2

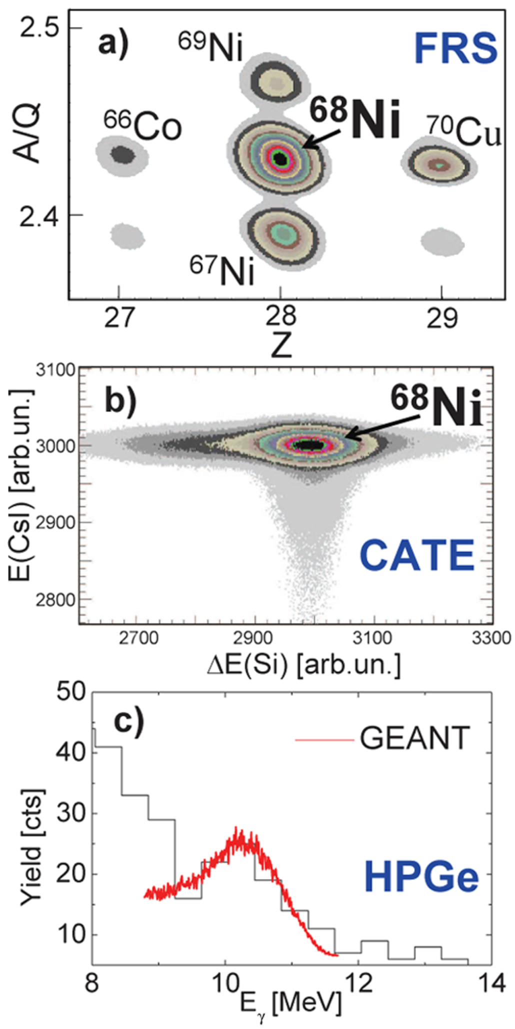

FIG. 1 (color online). In the upper panel (a) the fragments selected in the FRS are shown in a A/Q versus Z plot. The central panel (b) shows the E-ΔE spectra (from the CsI and Silicon detectors) of the outgoing beam detected after the target in the CATE calorimeter with selection of the incoming ^{68}Ni. In the lower panel (c) HPGe spectrum of the Cluster detectors after selecting incoming and outgoing ^{68}Ni and applying the Doppler correction for the projectile is shown. The continuous line is the result of a GEANT simulation for the in flight emission of a 11 MeV γ transition.

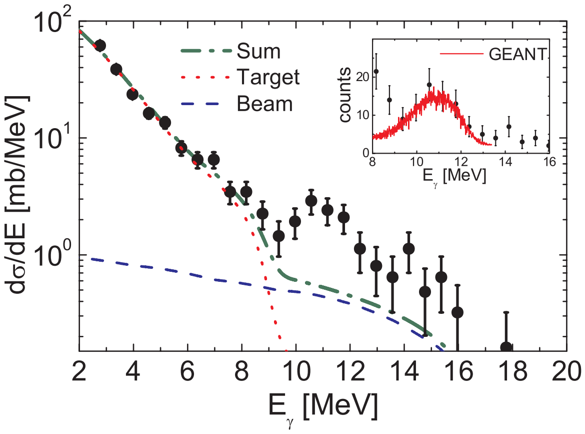

FIG. 2 (color online). The high-energy γ-ray spectrum measured with BaF_2 detectors and Doppler corrected with the velocity of the projectile. The lines are the statistical model calculations for the target (dotted line) and for the beam (dashed line) nuclei. In the inset the continuous line superimposed to the measured data is the result of a GEANT simulation for a γ-transition at 11 MeV.

detectors is shown in a linear scale together with the corresponding GEANT simulation. It is important to mention that for the HPGe detectors, being placed close to the CATE detector and having a time resolution >10 ns, the background reduction is not as good as for the BaF_2 detectors (placed backward and with a time resolution of <1 ns). For the spectra measured with BaF_2 detectors we have performed statistical model calculations [20] to interpret schematically the exponential part of the spectra. For the statistical calculation we have used the energy value given by the adiabatic cutoff energy of the Coulomb excitation process ($\approx$20 MeV). The adiabatic limit of Coulomb excitation was deduced with $E_{\max} \approx \frac{\hbar c \beta \gamma}{b_{\min}}$, where $b_{\min}$ is the smallest impact parameter for which interactions involving nuclear forces are negligible. The calculated statistical emission from the target and projectile was obtained using the standard GDR strength function, by correcting the γ-ray energy for the Doppler shift due to the projectile velocity (to be consistent with the experimental data treatment) and by folding with the detector response function. The condition of detecting only one γ ray can be neglected in the statistical model calculation because both the γ-ray efficiency ($\approx$5% at 1 MeV) and the γ multiplicity produced by the reaction (measured to be $\approx$1.1) are low. The statistical model predictions are shown in Fig. 2 in comparison with the data normalized at 3–5 MeV. One can note that the sum of the target and projectile statistical contributions reproduces remarkably well the exponential shape of the data and that there is an excess yield very pronounced at around 11 MeV, which can be attributed to the projectile emission on the basis of Doppler correction arguments. The data in the region of interest for searching the pygmy resonance in the electric dipole response function were obtained by subtracting from the measurements the computed statistical model contribution and some background extrapolated from the very high-energy region. The corresponding data are shown in the bottom panel of Fig. 3. The present results of the γ decay of the ^{68}Ni at 600 MeV/nucleon are characterized by a peak structure centered at 11 MeV for which it is important to understand not only the shape but also the measured value of the cross section. To describe the measured cross section for γ emission from the ^{68}Ni nucleus in the region $E_\gamma > 6$ MeV we have to evaluate the product of the excitation cross section σ^{exc} with the branching ratio for γ emission R_γ.

The γ-ray emission from the GDR is expected to be dominated by the ground state decay and the decay to the 2^+ state (due to the coupling of 1^- to 2^+) depends on the nuclear structure [21]. The latter for the pygmy, having a much smaller width (<1 MeV), is expected to be smaller. To verify this we have examined the 9–11 MeV region

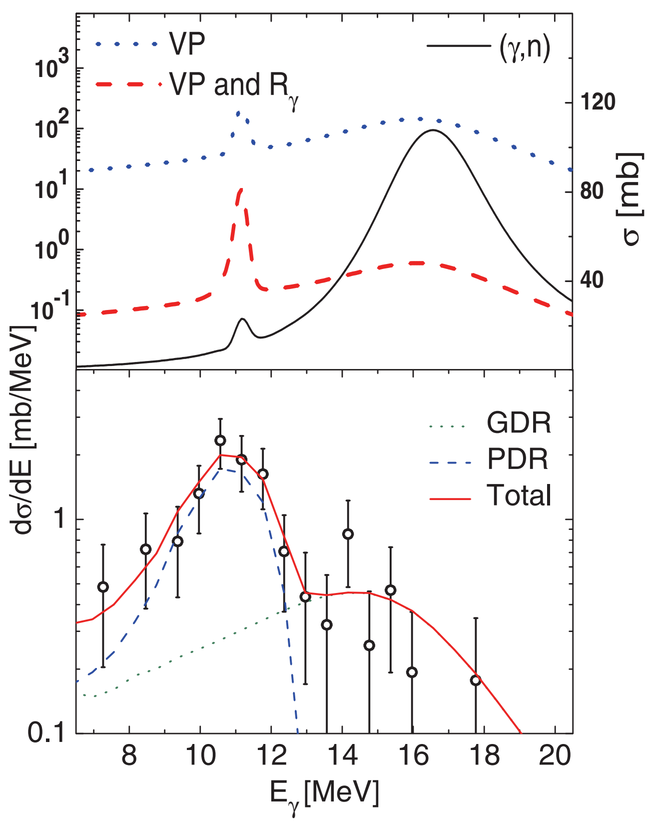

FIG. 3 (color online). In the upper part the ^{68}Ni photoabsorption cross section is shown with a full drawn line (scale on the right). The differential cross section obtained after applying the equivalent virtual photon method (VP) is shown with a dotted line (scale on the left). The dashed line (scale on the left) is obtained by including the γ branching ratio (VP and R_γ). In the bottom panel the open circles show the γ-ray cross section measured with BaF_2 detectors. The 3 lines in the bottom panel display calculations of the γ cross section (including the response function). The long dashed line is the decay of the PDR, the dotted line is the decay of the GDR and the thick line the sum of the two contributions.

when adding a possible component centered at 9 MeV (corresponding to the decay from the pygmy state to the 2^+ state at 2.033 MeV). This resulted in a worsening of the fit already with a contributions of 10%. The differential Coulomb excitation cross section for $E1$ multipolarity (integrated from a minimum impact parameter b_{min} to infinity [22]) is given by

$$\frac{d\sigma_{E1}}{dE_\gamma} = \sigma^{\mathrm{exc}} * R_\gamma = \left(\frac{1}{E_\gamma} N\sigma^{\mathrm{abs}}\right) * R_\gamma, \qquad (1)$$

where N is the equivalent virtual photon number for pure Coulomb excitation and σ^{abs} is the photonuclear cross section with multipolarity $E1$. From expression (1) one can see that indeed the γ energy and virtual photon number factors produce an excitation cross section characterized by a sizable distortion of the electric dipole response function. This point is illustrated in the top panel of Fig. 3. In this figure an electric dipole response function with a small peak at 11 MeV with 5% of the energy weighted sum rule strength (EWSR) is shown. The corresponding $\frac{1}{E_\gamma} N\sigma^{\mathrm{abs}}$ is shown in the same figure with the dotted line. The virtual photon number was evaluated by choosing as minimum impact parameter for Coulomb excited nuclei $b_{\mathrm{min}} = 12.85$ fm from the systematics of Benesh *et al.* [23]. The comparison of the continuous and dotted lines shows clearly how the large flux of virtual photons at the lowest energy enhances, as expected, the intensity of the electric dipole response in the pygmy region. The additional and very important effect of R_γ is displayed with dashed line curve. For the evaluation of R_γ the procedure described in Refs. [24,25] has been adopted. In particular R_γ is due to two contributions $R_\gamma = R_\gamma^{\mathrm{dir}} + R_\gamma^{\mathrm{CN}}$, where R_γ^{dir} is the direct decay contribution while R_γ^{CN} is the decay after the resonance had coupled to the compound nucleus states at the same excitation energy. This latter contribution depends on the nuclear level density. For the calculation shown with dashed line in Fig. 3 the adopted level density is based on the shell model Monte Carlo calculation [26]. Using this level density the total γ branching ratio is found to be $\approx 0.4\%$ and $\approx 4\%$ for the region of the GDR and the PDR, respectively. The present values are consistent with the total photon branch integrated over the energy interval 9.5–25 MeV of the heavier ^{208}Pb ($R_\gamma \approx 2\%$) [24]. The detector response function was folded to the dashed curve of Fig. 3 and the corresponding result is shown in the bottom panel. There is a remarkable agreement of the calculated cross section with the data both in size and shape when one assumes an electric dipole strength function with $\approx$5% of EWSR strength at 11 MeV [the corresponding $B(E1)$ value being 1.2 e^2 fm^2]. In contrast, a calculation assuming a standard Lorentzian function, presented as a short dashed line in the bottom panel of Fig. 3 produces a spectral shape and size of the cross section which differs from the data by approximately 1 order of magnitude in the region below 12 MeV. Theoretical predictions are available for the pygmy resonance for neutron-rich nuclei such as Sn and Ni isotopes [9–11,27]. In particular, for the ^{68}Ni nucleus, recent calculations within the relativistic random phase approximation (RRPA) model [9] and the quasiparticle relativistic random phase (QRRPA) model [10] predict at 9–10 MeV a pygmy structure with a EWSR strength of 4% and 10%, respectively. For the analysis of the present data an assumption of 9% of the EWSR strength in the pygmy region could fit the data if the used value of the level density is a simple extrapolation from stable nuclei. The level density value from stable nuclei is a factor of $\approx$5 larger of that used in the calculation of Fig. 3 taken from more accurate calculations [26]. The interesting result here obtained on the strength of the pygmy resonance (5% to 9% of the EWSR strength) calls for experiments on level density measurements in exotic nuclei to pin down with smaller uncertainty the $E1$ strength.

In summary, we have here presented the first experimental search of a pygmy resonance in the neutron-rich ^{68}Ni nucleus using the virtual photon scattering technique. Evidence is found for the presence of sizeable strength energetically located below the GDR and centered at $\approx$11 MeV with approximately 5% of the EWSR strength. This is similar to what has been found in unstable neutron-rich ^{132}Sn [8], but is sizably larger than in stable nuclei. This result is in rather good agreement with theoretical predictions and provides relevant information which can be related to neutron skin and nuclear symmetry energy [4]. The present result for the ground state γ decay from the pygmy resonance opens interesting future perspectives with more intense radioactive beams and further improved instrumentation for γ detection at relativistic energies such as the AGATA γ-ray tracking array. In fact, it will be very interesting for the study of neutron skin in nuclei far from stability to measure more in detail and systematically the structure of the electric dipole response in an energy interval larger than that of the present experiment.

This work was partially supported by the Italian Istituto Nazionale di Fisica Nucleare and by the Polish Ministry of Science and Higher Education Grants No. 1 P03B 03030.

*Present address: Universidad Autonoma de Madrid, E-28049 Madrid, Spain.
†Present address: RIKEN, Wako, Saitama 351-0198, Japan.
‡Present address: Univerisité Paris-sud and IPN Orsay, F-91406 Orsay Cedex, France.
§Present address: University of Oslo, NO-0317 Oslo, Norway.

[1] S. Goriely, Phys. Lett. B **436**, 10 (1998); S. Goriely and E. Khan, Nucl. Phys. **A706**, 217 (2002).
[2] G. A. Bartholomew, *et al.*, Adv. Nucl. Phys. **7**, 229 (1973).
[3] T. Hartmann *et al.*, Phys. Rev. Lett. **93**, 192501 (2004).
[4] A. Klimkiewicz *et al.*, Phys. Rev. C **76**, 051603 (2007).
[5] J. Piekarewicz Phys. Rev. C **73**, 044325 (2006).

[6] A. Leistenschneider *et al.*, Phys. Rev. Lett. **86**, 5442 (2001).
[7] E. Tryggestad *et al.*, Phys. Lett. B **541**, 52 (2002).
[8] P. Adrich *et al.*, Phys. Rev. Lett. **95**, 132501 (2005).
[9] D. Vretenar *et al.*, Nucl. Phys. **A692**, 496 (2001).
[10] L. Cao and Z. Ma, Mod. Phys. Lett. A **19**, No. 38, 2845 (2004).
[11] N. Paar *et al.*, Rep. Prog. Phys. **70** 691 (2007).
[12] T. Aumann, Eur. Phys. J. A **26**, 441 (2005).
[13] H. Geissel *et al.*, Nucl. Instrum. Methods Phys. Res., Sect. B **70**, 286 (1992).
[14] H.J. Wollersheim *et al.*, Nucl. Instrum. Methods Phys. Res., Sect. A **537**, 637 (2005).
[15] R. Lozeva *et al.*, Nucl. Instrum. Methods Phys. Res., Sect. A **562**, 298 (2006).
[16] G. de Angelis, A. Bracco, and D. Curien, Europhysics News **34**, 181 (2003).
[17] J. Eberth *et al.*, Prog. Part. Nucl. Phys. **46**, 389 (2001).
[18] O. Wieland *et al.*, Phys. Rev. Lett. **97**, 012501 (2006); A. Bracco *et al.*, Mod. Phys. Lett. A**22**, No. 33, 2479 (2007).
[19] R. Brun *et al.*, CERN Report No. CERN-DD/EE/84-1.
[20] I. Dioszegi *et al.*, Phys. Rev. C **63**, 047601 (2001).
[21] V. Yu. Ponomarev and A. Krasznahorkay, Nucl. Phys. A **550**, 150 (1992).
[22] C. Bertulani and G. Baur, Phys. Rep. **163**, 299 (1988), and references therein.
[23] C. Benesh, B. Cook, and J. Vary, Phys. Rev. C **40**, 1198 (1989).
[24] J.R. Beene *et al.*, Phys. Rev. C **41**, 920 (1990).
[25] J.R. Beene, G.F. Bertsch, P.F. Bortignon, and R.A. Broglia Phys. Lett. B **164**, 19 (1985).
[26] Y. Alhassid *et al.*, Phys. Rev. Lett. **99**, 162504 (2007); C.N. Gilbreth and Y. Alhassid (private communication).
[27] D. Sarchi *et al.*, Phys. Lett. B **601**, 27 (2004).